Testing the Environmental Dependence of the Luminosity-Halo Maximum Circular Velocity Relation from Abundance Matching

Radu Dragomir

November 4, 2016

A Thesis Submitted in Partial Satisfaction
Of the Requirements for the Degree of
Bachelor of Science in Physics
at the
University of California, Santa Cruz

The thesis of Radu Dragomir is approved by:

Joel R. Primack	David P. Belanger
Thesis Advisor	Theses Coordinator

Robert Johnson
Chair, Department of Physics

Abstract

The rapid progression in both the theoretical and observational aspects to understanding galaxy formation elicits intrigue towards their connection and whether it remains constant with environment. We construct a mock luminosity catalog by abundance matching halo velocities from the Bolshoi-Planck simulation with luminosities from SDSS and check that the mock data are consistent with observations. We then investigate the galaxy-halo luminosity connection in nine different density environments and find no environmental dependence with r band magnitudes when probing at 8 and 16 Mpc scales and the same for the g band at the 8 Mpc scale. However, there is deviation for the galaxy-halo connection at the bright end for u band magnitudes on the 8 Mpc scale, especially in the most dense and also the least dense environments. Predictions on galaxy formation are then offered at nine different density environments through the mock galaxy mass accretion rates and concentrations and how they evolve with r-band magnitudes. We find that at brighter magnitudes mass accretion rates at higher density environments are more dominant, while higher at the faint end for less dense regions.

Contents

Acknowledgments

I would like to thank Joel Primack for introducing me to the world of research in theoretical astrophysics. It has been my dream to be involved with solving the mysteries of the universe, as with my work in studying dark matter properties. I would also like to thank Aldo Rodriguez-Puebla for his guidance throughout this entire project. It was Aldo who kindly provided all the knowledge and support that I needed to perform the tasks required for this thesis.

1 Introduction

Understanding galaxy formation and evolution in the universe is an extensive effort in modern astronomy. In the standard model of cosmology, known as ΛCDM, there is an ample amount of evidence that galaxies form and evolve in halos composed of cold dark matter (CDM). To cite one example, the existence of dark matter (DM) is necessary to arbitrate the discrepancy between observations and Keplerian expectations of stellar orbits in galaxies. Under our current understanding of the structure formation paradigm, cold dark matter constitutes 25.9%, dark energy is 69.3%, and ordinary baryonic matter composes 4.8% of the universe based on the latest analysis of the Planck Collaboration. According to this model, CDM halos evolve by the accretion of material into halos and through mergers with other halos while at the same time galaxy formation and evolution takes place under the various astrophysical processes that ultimately shape their observed properties. Naturally, it is expected that the observed properties of galaxies should be closely related to the properties and evolution of dark matter halos.

From the theoretical point of view, the formation and evolution of the key properties of dark matter halos are very well understood through the use of cosmological simulations. From this perspective, studying the observed properties of galaxies through the galaxy-halo connection is of great convenience to understand and constrain the key astrophysical process that could play a main role during the formation and evolution of the galaxies. In this direction, statistical approaches to connect galaxies with their host halos are not only a simple but also a powerful alternative to study how galaxies and halos coevolve.

Galaxy formation can be also studied by using more complex methods. For example, hydrodynamical simulations of galaxy formation provide a powerful technique for calculating the non-linear evolution of cosmic structure formation while at the same describing the formation of a galaxy. Apart from hydrodynamical simulations, semi-analytical models try to solve the equations describing the formation of galaxies by using approximate analytic techniques. The main disadvantages of the above methods is that hydrodynamical simulations

are extremely expensive to run computationally. Furthermore, the complexity and degeneracy on the parameters used in semi-analytical models lead to a great degree of uncertainty in the modeling.

The main advantage of statistical approaches is that they are powerful methods because we do not require any initial knowledge of galaxy evolution, i.e., galaxy formation can be studied in an empirical basis. Moreover, these models can be used to constrain the more complex approaches as those described above. The statistical approach we use in this paper is abundance matching.

Abundance matching is a technique in which the observed galaxy number density for a given property is matched to the theoretical halo number density, resulting in an output of an empirical correlation between galaxy and halo properties. The most popular properties employed in the literature are luminosities for galaxies and the maximum circular velocities of the halos. Several authors have found that abundance matching, i.e., the luminosity-maximum circular velocity relationship, predicts galaxy clustering that is in excellent agreement with observed data. However, a common assumption in the literature is that galaxy luminosities only depend on the maximum circular velocities of the halos.

Our main goal is to determine whether the connection between the galaxy luminosity to halo maximum circular velocity relation from abundance matching has a dependence on the environment. As mentioned above, previous studies have assumed that this relation is independent of environment, and we will be the first to test whether this is true. In reality, this relation is expected to depend on environment because the properties of the galaxies might be determined by different halo properties that depend on some environmental factor. We will test this by studying the dependence of the luminosity function with environment and compare to the predictions when the galaxy luminosity to halo maximum circular velocity relation is assumed to be universal. With higher resolution simulations and observations advancing in better instrumentation, it is important to connect the data between both fronts that are progressing towards understanding galaxy formation. If the galaxy-halo luminosity

connection reproduces observations, remaining constant with environment, then we can conclude that the relation is appropriate to use for acquiring predictions on galaxy formation. A universal relation would also imply that there is a single halo property to understand galaxy formation.

2 Methods

2.1 The Bolshoi-Planck Simulation

To study the environmental dependence of the galaxy-halo connection, in this paper we will use a very high resolution (1 kpc) N-body cosmological simulation, the Bolshoi Plank simulation (BolshoiP). This simulation has 2048^3 DM particles, each of mass $1.9 \cdot 10^8 M_\odot$/h, in a box of side length 250 Mpc/h (with the Hubble parameter $h = 0.678$). This simulation was run on the Pleiades supercomputer and uses cosmological parameters from the Planck satellite. Halos/subhalos and their merger trees were calculated with the phase-space temporal halo finder ROCKSTAR [1][2]. Halo masses were defined using spherical overdensities according to the redshift-dependent virial overdensity $\Delta_{\rm vir}(z)$ given by the spherical collapse model [3], with $\Delta_{\rm vir}(z) = 333$ at $z = 0$. The Bolshoi-Planck simulation is complete down to halos of maximum circular velocity $v_{\rm max} \sim 55$ km/s. Many properties in the simulation have been analyzed through the ROCKSTAR code, but we still have a surplus of data waiting to be analyzed. Our main goal here is to study the distribution of galaxies through the distribution of dark matter halos via abundance matching.

2.2 Determining the Luminosity-V_{max} Relation

Abundance matching is a simple approach relating a halo property, such as mass or maximum circular velocity, to that of a galaxy property, such as luminosity or stellar mass. As a result, abundance matching gives a galaxy-halo relation. In its most simple form the number density distribution of the halo property is matched to that of the galaxy property to obtain the

relation. Note that abundance matching assumes that that there is a one-to-one monotonic relationship between galaxies and halos with some scatter. This is actually not surprising since, as for galaxies, the most abundant halos are least massive. In this paper we choose to relate galaxy luminosities, L, to halo maximum circular velocities V_{max} as

$$\int_{L}^{\infty} \phi_{gal}(L')dL = \int_{V_{max}}^{\infty} \phi_h(V'_{max})dV_{max}, \tag{1}$$

in which $\phi_{gal}(L')$ and $\phi_h(V'_{max})$ represent the differential form of the density distribution function to their respective properties, i.e., the luminosity and velocity functions respectively. Figure 1 illustrates the application of abundance matching by relating galaxy's luminosity with a halo's mass by using a similar equation. Normally, halo masses are used but recent studies have found that halo maximum circular velocities are more fundamental to connect halos to galaxies [5]. This figure shows that by equating the abundances between galaxy luminosity to the abundances of halo mass it is possible to obtain the corresponding luminosity-halo mass relation and thus the mass-to-light ratio as indicated in the inset figure. To construct a mock galaxy catalog of luminosities from the Bolshoi-Planck simulation we apply the above procedure for every halo in the simulation by matching the halo velocity function and the galaxy luminosity function.

2.3 Inputs for Abundance Matching

2.3.1 The V_{max} Halo Distribution

Previous studies have found that the maximum circular velocity of distinct dark matter halos (those that are not contained in bigger halos) is the halo property that correlates better with galaxy luminosity. For subhalos (halos that are contained in bigger halos), however, [5] found the highest maximum circular velocity reached along the halos main progenitor branch correlates better with galaxy luminosity by comparing to observations of galaxy clustering. The motivation behind this is that subhalos can lose mass once they fall into a larger halo.

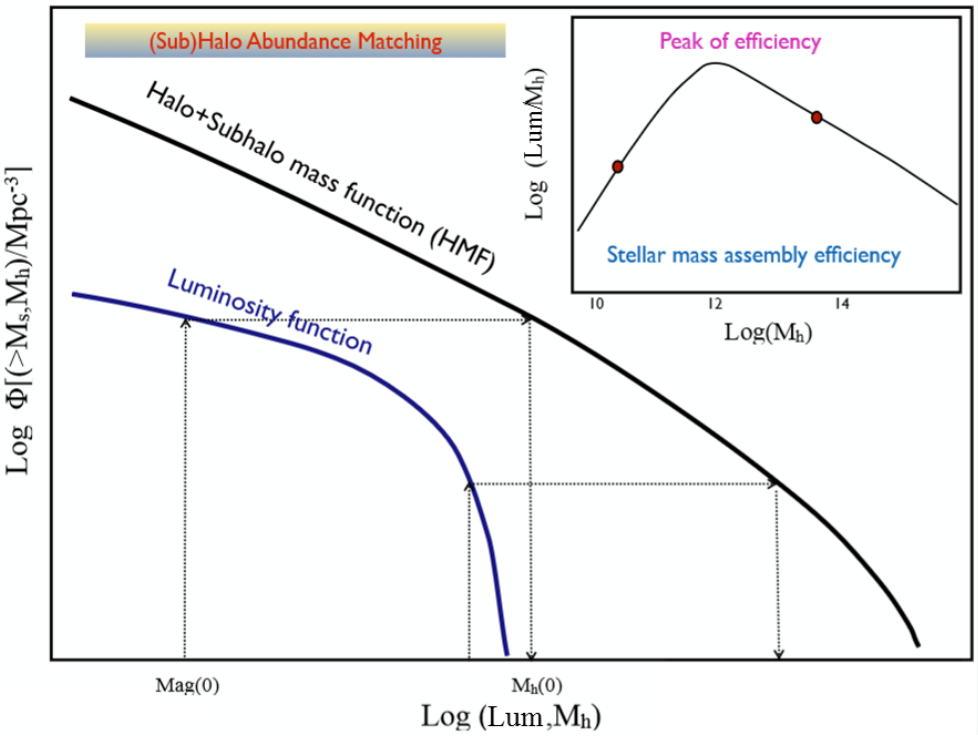

Figure 1: We obtain abundances from each the galaxy luminosity function and the halo mass function. We take some galaxy magnitude's cumulative number and find at which halo mass this abundance occurs, and repeat for all magnitudes. Then we can obtain a relation between the galaxy luminosities and halo masses [4].

In the following equation, we use

$$V_{\rm max} = \begin{cases} V_{\rm max} & \text{Distinct halos} \\ V_{\rm peak} & \text{Subhalos.} \end{cases} \tag{2}$$

as the halo proxies for galaxy luminosity, where $V_{\rm peak}$ is the maximum circular velocity throughout the entire history of a subhalo and $V_{\rm max}$ is at the observed time for halos. The velocity function (VF) is defined as the number of halos per comoving volume per unit of $V_{\rm max}$. In this paper, we use the parameterized VF from [6] which is a very accurate fit to a suite of very high resolution of N-body cosmological simulations. The functional form

obtained in [6] is

$$\frac{dn_{\rm halo}}{dV_{\rm max}} = AV_{max}^2 \left[\left(\frac{V_{\rm max}}{V_0} \right)^{-a} + 1 \right] exp \left[- \left(\frac{V_{\rm max}}{V_0} \right)^{-b} \right], \tag{3}$$

where the redshift dependent parameters $\chi_i = log(a/E(z)), a, b,$ and $logV_0$ for Eq. 3 have the form

$$\chi_i = \chi_{0,i} + \chi_{1,i} z^{\alpha_1} + \chi_{2,i} z^{\alpha_2}, \tag{4}$$

and the best fit parameters are given in Table 1.

χ_i	$\chi_{0,i}$	$\chi_{1,i}$	$\chi_{2,i}$	α_1	α_2
$\log(A/E(z))$	4.785	-0.207	0.011	0.897	1.856
a	-1.120	0.394	0.306	0.081	0.554
b	1.883	-0.146	0.005	1	2
$\log V_0$	2.941	-0.169	0.002	1	2

Table 1: Best fit parameters to use in Eq. 3 for the halo maximum circular velocity function. Though the best fit parameters are redshift dependent, in this paper the focus is on the nearby universe $z = 0$ so the expansion rate $E = 1$ and only the constant terms are needed in Eq. 4. From [6], recall that for subhalos $V_{\rm max} = V_{\rm peak}$ was parameterized such that it is proportional to that of halos, so the VF of subhalos is

$$\frac{dn_{\rm sub}}{dlog(V_{\rm peak})} = C_{sub}(z) G(V_{\rm peak}, z) \frac{dn_{\rm halo}}{dlog(V_{\rm max})}, \tag{5}$$

where

$$C_{sub}(z) = C_0 + C_1 a + C_2 a^2 + C_3 a^3 + C_4 a^4, \tag{6}$$

and

$$G(V_{\rm peak}, z) = X^{\alpha_{sub,1}} exp(-X^{\alpha_{sub,1}}), \tag{7}$$

with $X = V_{\rm peak}/V_{cut}(z)$ in which we have the function fit form

$$log(V_{cut}(z)) = V_0 + V_1 z + V_2 z^2 + V_3 z^3 + V_4 z^4, \tag{8}$$

and the parameters for Eq. 6 to Eq. 8 are given in Table 2.

Param.	V_{acc}	V_{peak}
C_0	-0.6768	-0.5800
C_1	1.3098	1.5905
C_2	-1.1288	-1.1360
C_3	0.0090	-0.0378
C_4	0.214820	0.18092
$\alpha_{sub,1}$	1.1375	1.1583
$\alpha_{sub,1}$	0.5200	0.5806
V_0	0.2595	0.5410
V_1	3.5144	3.4335
V_2	-2.8817	-3.0026
V_3	-0.3910	-0.3687
V_4	0.8729	0.9450

Table 2: Best fit parameters to use in Eq. 6 through 8 for the subhalo maximum circular velocity function with velocities measured in km s^{-1}.

We calculate the total VF by adding the halo and subhalo VFs which are $dn_{\rm halo}/d\log(V_{\rm max})$ and $dn_{\rm sub}/d\log(V_{\rm peak})$, respectively. For illustrative purposes, Fig. 2 shows the total VF as a function of z for $z = 0, 2, 4, 6, 8$. Recall that in this paper we will focus mainly at $z = 0$ but we might extend our study in future work to higher redshifts.

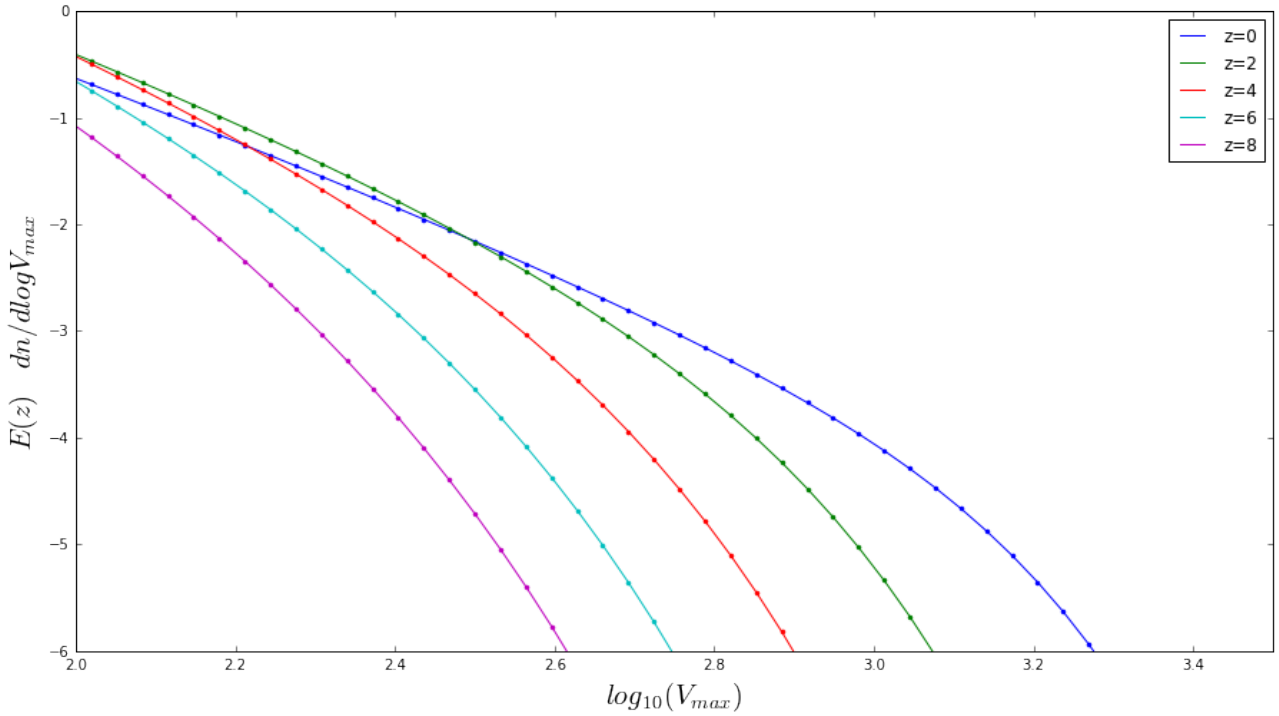

Figure 2: For redshift z = 0, 2, 4, 6, and 8 we have the maximum central velocity function of halos, E * dn/dVmax vs V_{max} on logarithmic axes.

2.3.2 The Luminosity Function

In this section we describe the luminosity functions (LFs) employed for abundance matching. The luminosity function is defined as the number of galaxies per comoving volume per magnitude. Here we use LFs in the u, g and r bands of the Sloan Digital Sky Surveys (SDSS), kindly provided by Aldo Rodriguez-Puebla. These luminosity functions were carefully constructed by using a sample of galaxies from a local volume ($0.0033 < z < 0.05$) to study very low mass/luminosity galaxies [7]. Additionally, these LFs have been corrected to account for missing galaxies due to surface brightness limits in the SDSS. In order to avoid sample and Poisson variance, these LFs were also recalculated by using a second galaxy sample which consists (on the main galaxy sample) of the SDSS DR7 with $\sim 650,000$ galaxies over 7748 deg^2. compromising the redshift range between $0.01 < z < 0.2$. Thus, the resulting LFs are a combination of a local sample, excellent to study very low mass/luminosity galaxies, and of a larger and more distant sample to complete and avoid any sample variance on the high

end of the LFs. These LFs are excellent tools for studying a very large dynamical range. In this paper we find the best fitting functions to the u, g and r bands of the LFs. Previous studies have found that single Schechter function seems to be consistent with observations [8]. A Schechter function is totally defined by three parameters, having the form

$$\phi(M) = \frac{\ln 10}{2.5}\phi^* 10^{0.4(M^*-M)(1+\alpha)} \exp\left(-10^{0.4(M^*-M)}\right) \tag{9}$$

where M^* is the characteristic luminosity where the functions change from a power law to an exponential decay, ϕ^* is the normalization of the function which has units of number density, and α the slope of the power-law range.

However, more recent detailed studies have questioned the above, finding that a double Schechter function is more accurate for the description of the LFs in addition of finding more shallower slopes at the high luminosity end instead of an exponential decay. Therefore, in this paper we choose to use LFs that are described by a function composed of a single Schechter function plus another Schechter function with a subexponential decay for the u, g and r bands, which is

$$\begin{aligned}\phi(M) = &\frac{\ln 10}{2.5}\phi_1^* 10^{0.4(M_1^*-M)(1+\alpha_1)} \exp\left(-10^{0.4\left(M_1^*-M\right)\beta_1}\right) \\ &+\frac{\ln 10}{2.5}\phi_2^* 10^{0.4(M_2^*-M)(1+\alpha_2)} \exp\left(-10^{0.4\left(M_2^*-M\right)\beta_2}\right).\end{aligned} \tag{10}$$

The parameters for the r, g, and u bands are given in Table 3. The total LFs for each band are shown in Fig. 3 from both observations (circle markers) and the fitting functions (solid lines). Magnitudes are increasing in brightness towards the right, and abundances increase towards the top. We can see that our proposed function in Eq. 10 accurately describes the observations in the r, g, and u bands.

Band	M_1^*	α_1	β_1	$log10(\phi)_1$	M_2^*	α_2	β_2	$log10(\phi)_2$
u	-17.7805	-0.577162	1	-1.5749	-11.5607	-1.00881	0.28859	-0.201578
g	-20.2124	-1.54755	1	-2.35423	-17.9455	0.0544511	0.623114	-1.97345
r	-21.033	-1.49327	1	-2.4128	-18.3412	0.14242	0.583125	-2.10106

Table 3: Parameters in each band for the Schechter function LF's [7].

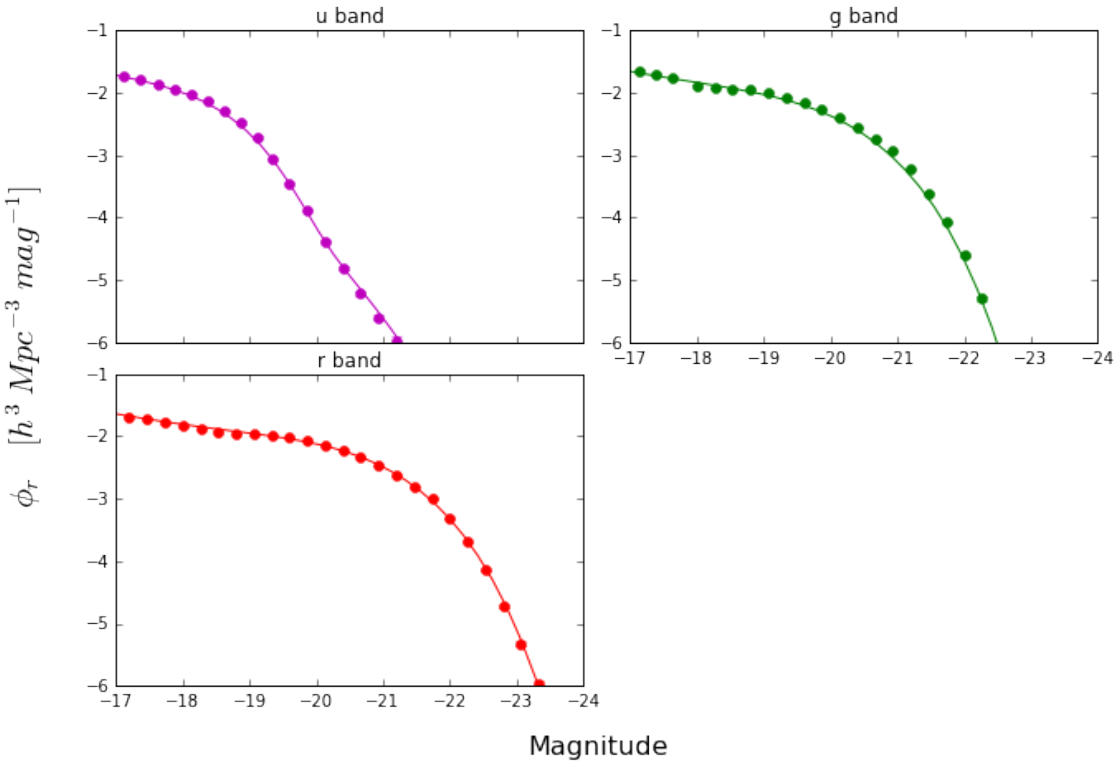

Figure 3: Luminosity functions for u, g, and r bands by using Eq. 10 with parameters tabulated in Table 3 (solid lines), along with observations (circle markers).

2.4 The Luminosity-$V_{\max}$ Relation

In this section we describe how we obtain our luminosity-$V_{\max}$ relationships in the u, g and r bands from abundance matching. We begin by integrating the total VF distribution from some value of $V_{\max}$ out to infinity to obtain the cumulative number VF. We calculate the cumulative VF from 35 km/s to 2000 km/s by taking fifty velocity bins of equal increments

in the logarithmic space. We then solve Eq. 1 by finding the corresponding galaxy luminosity for a given $V_{\rm max}$ using the bisection method and find the resulting luminosity-V_{max} relationships for the fifty bins. We do the same for every band. With these relationships, we are then able to convert directly from velocities to luminosities in each band to construct a mock catalog using the Bolshoi-Planck simulation.

Once we have the luminosity-$V_{\rm max}$ relationships, we tabulated these relations into a separate file. We then use cubic spline interpolation to obtain the closest function from velocities to luminosities in BolshoiP. Here we input $V_{\rm max}$ for distinct halos while for subhalos we input $V_{\rm peak}$, see Eq. 2, from our sample of 2659847 halos and subhalos from BolshoiP to obtain mock luminosity magnitudes in the r, g, and u bands. These mock magnitudes could now be used in LFs to compare with observations. The relationships between velocities and magnitudes in each band are shown in Fig. 4. In this figure, we observe that there is a systematic rollover near $\log V_{\rm max} \sim 2.3$, i.e., $V_{\rm max} \sim 200$ in all the relations which approximately corresponds to Milky-Way sized galaxies and also approximately represents the line between star forming and quenched galaxies.

2.5 Luminosity Functions by Environment

As mentioned in the introduction, our main goal is to determine whether the connection between the galaxy luminosity to halo maximum circular velocity relation from abundance matching has a dependence on the density environment. Our strategy is to assume that the relation is *independent* of environment for which our mock catalogs as described above would make strong predictions regarding the abundance of galaxies as a function on their environment. We are particularly interested to test this in different bands. Theoretically, it is predicted that stellar mass is the galaxy property that correlates better with halo mass, thus the reason of studying different bands is that while redder bands (r-band) would trace much better stellar mass and perhaps be less sensitive to large scale environment, ultraviolet bands (u-bands) trace better the star-formation rates in galaxies. It is a well established

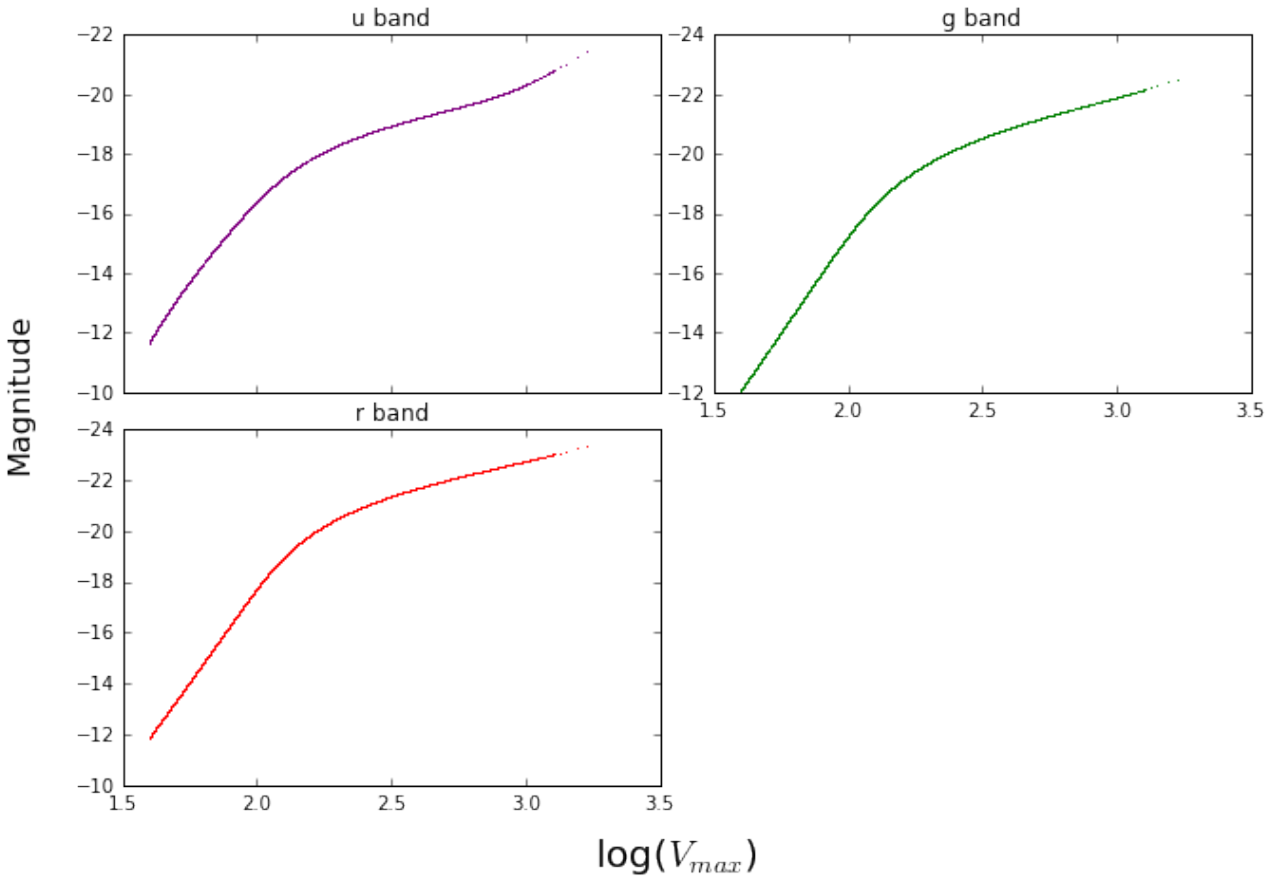

Figure 4: The relation between maximum central velocities from halos in BolshoiP and observed magnitudes in the r (red), g (green), and u (purple) bands, found by using abundance matching.

observation that star-forming galaxies with young stars producing UV and blue light are more likely to be found in less dense environments while red galaxies with older stars are more likely to be found in denser environments. Based on that, we expect that as we go towards more ultraviolet bands, the assumption that the galaxy luminosity to halo maximum circular velocity relation with environment should break.

Next, we define our proxy for environment in our mock galaxies for BolshoiP. We begin by defining a sample of galaxies to use as tracers for environment. We choose galaxies that range from -21.8 to -20.1 magnitudes in the $r-$band. We note that our definition of environment would not depend on our tracers but we chose this particular range given that the number of galaxies in observations is maximized. We will define the environment by counting the

number of all neighboring galaxies with ranges from -21.8 to -20.1 magnitudes in the $r-$band by centering spheres of 8 Mpc in every galaxy and calculate

$$\delta_8 = \frac{\rho - \bar{\rho}}{\bar{\rho}}. \tag{11}$$

Here ρ is the number density within the sphere of 8 Mpc and $\bar{\rho}$ is the average number density within the whole box of side length 250 Mpc/h. Following [9], we separate galaxies by using the same density environments used in that paper. The divisions are shown in Table 4 along with effective volume fractions in the simulation (which also must be considered). We perform a Monte-Carlo integration for the 2659847 halos and subhalos, and find the volume fraction for each of the nine density environments occupied by placing the same number of randomly distributed galaxies in the 250 Mpc length box [10]. The volume fraction of each region is the number of galaxies in that region divided by the total number of galaxies. We thus calculate the luminosity function for each density environment as

$$\Phi = \frac{N}{250^3 f \delta M}, \tag{12}$$

where f is the volume fraction of each density environment listed in Table 4, and N is the number of halos in each magnitude bin of width δM. Here, δM is the difference between the maximum and minimum magnitude divided by 30 which is the number of bins. In this way, we have the galaxy LF from our mock galaxy catalog to compare to observations for each density region. Additionally, by maintaining galaxies in the same environments calculated from the r-band (with the same volume fractions), we calculate their LF's for each density environment by using their u and g band magnitudes. We will also calculate environments by using spheres of size 16 Mpc, though we only compare the r band LF's with observations for the sphere of 16 Mpc. As we will argue below, the reason for this is that the 16 Mpc scale is not very reliable to probe in underdense and overdense regions.

region	$\delta_{8,16}$ min	$\delta_{8,16}$ max	f_8	f_{16}
d1	-1.00	-0.75	0.2553	0.0573
d2	-0.75	-0.55	0.1554	0.1418
d3	-0.55	-0.40	0.0864	0.1255
d4	-0.40	0.00	0.1640	0.3050
d5	0.00	0.70	0.1670	0.2701
d6	0.70	1.60	0.1022	0.0881
d7	1.60	2.90	0.0453	0.0118
d8	2.90	4.00	0.0136	0.0005
d9	4.00	∞	0.0108	0.0

Table 4: Bounds in density contrasts for each region, along with the volume fractions done for both sphere sizes of 8 and 16 Mpc calculated from the r-band.

3 Results

In this paper we compared our predicted LFs based on our environment independent luminosity to halo maximum circular velocity relationships from abundance matching to observations. Measurements to observations were carried out by Aldo Rodriguez by using the SDSS DR7 galaxy catalog with environments calculated in a similar way as described above. The counts for observed samples are required to be corrected for incompleteness, conversely to mock data. The LFs were executed for galaxies with spectroscopic redshifts with $z < 0.1$. Magnitudes were $K-$ and evolution corrected at a rest-frame $z = 0$ using $K-$correct [11]. We begin by describing the LFs calculated in the r-band and with environments calculated on spheres of 8 Mpc scales. Figure 5 shows the predicted BolshoiP mock LFs compared to the SDSS LFs shown as the solid lines and filled circles, respectively. The different colors show the resulting LFs from the various environments in 8 Mpc sphere scales as tabulated in Table 4. The shaded areas show the Poissonian errors from the mock catalog calculated as the square

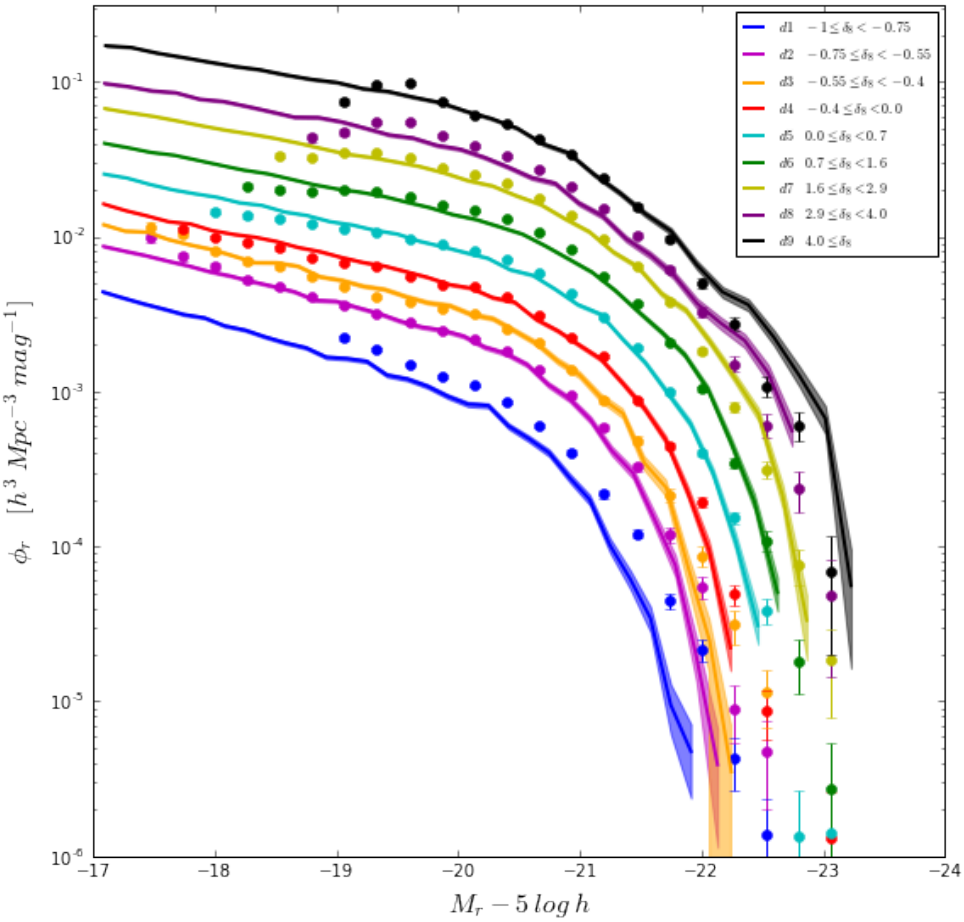

Figure 5: A comparison of BolshoiP mock LFs (solid lines) with SDSS LFs (circle markers) in 9 different density environments on the 8 Mpc scale, using r-band magnitudes.

root of the counts. Approximately, the environments shown in Fig. 5 and tabulated in Table 4 range from undense regions d_1 corresponding to voids to very high density environments d_9 corresponding to clusters. We begin by noting the excellent agreement between our mock data and observations since our predicted LFs seems to globally reproduce the correct trend with environment. Recall that the main assumption in our model is that the luminosity to halo maximum circular velocity relation is the same on every environment. Both for the BolshoiP simulation and observations show that the luminosity function is very well described by a Schechter function (see also [9]), that is, the LFs can be very well described by a power law at low luminosities and by an exponential decay at high luminosities.

Figure 6 shows again the the predicted BolshoiP mock LFs compared to the SDSS LFs in the

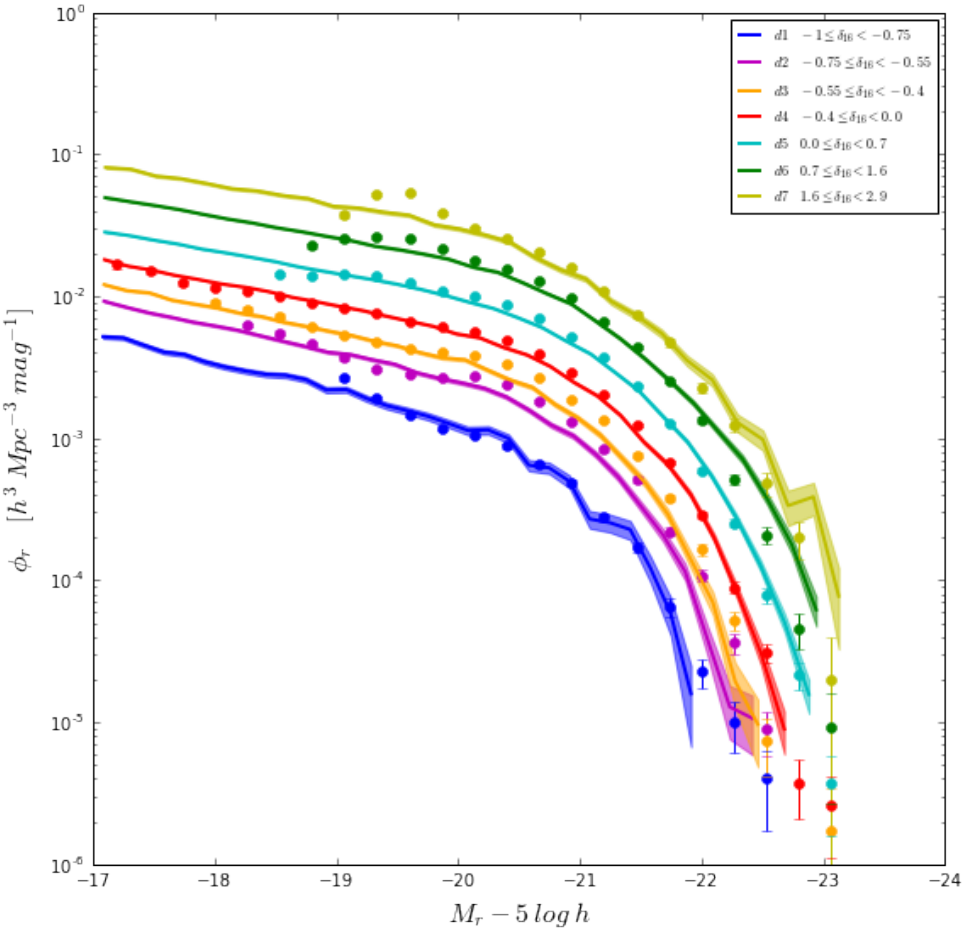

Figure 6: A comparison of BolshoiP mock LFs (solid lines) with SDSS LFs (circle markers) in 9 different density environments on the 16 Mpc scale, using r-band magnitudes.

r-band but this time for environments in 16 Mpc spheres scales, see Table 4. In this case we also find a remarkable agreement with observations. Similarly to when environments were calculated in spheres of 8 Mpc, here we find that Schechter functions accurately describe both mock LFs and the observational data. Note that the range of density environments is different from above, i.e., environments d_8 and d_9 where omitted. The reason is that using larger spheres invokes a tendency to find more average environments, where a high density would be difficult to measure. Here we find that density bins below d_7 are robust enough to make a comparison to observations. In other words, on the 16 Mpc scale the universe looks more homogeneous so most of the galaxies selected in different environments for the case of the 8 Mpc scale would migrate from low and high to more median density

environments. Therefore, the 16 Mpc scale is not very reliable to probe in underdense and overdense regions. Thus, we exclude the two most overdense regions since they have small volume fractions on the 16 Mpc scale. However, interesting results could still be obtained for these median density regions.

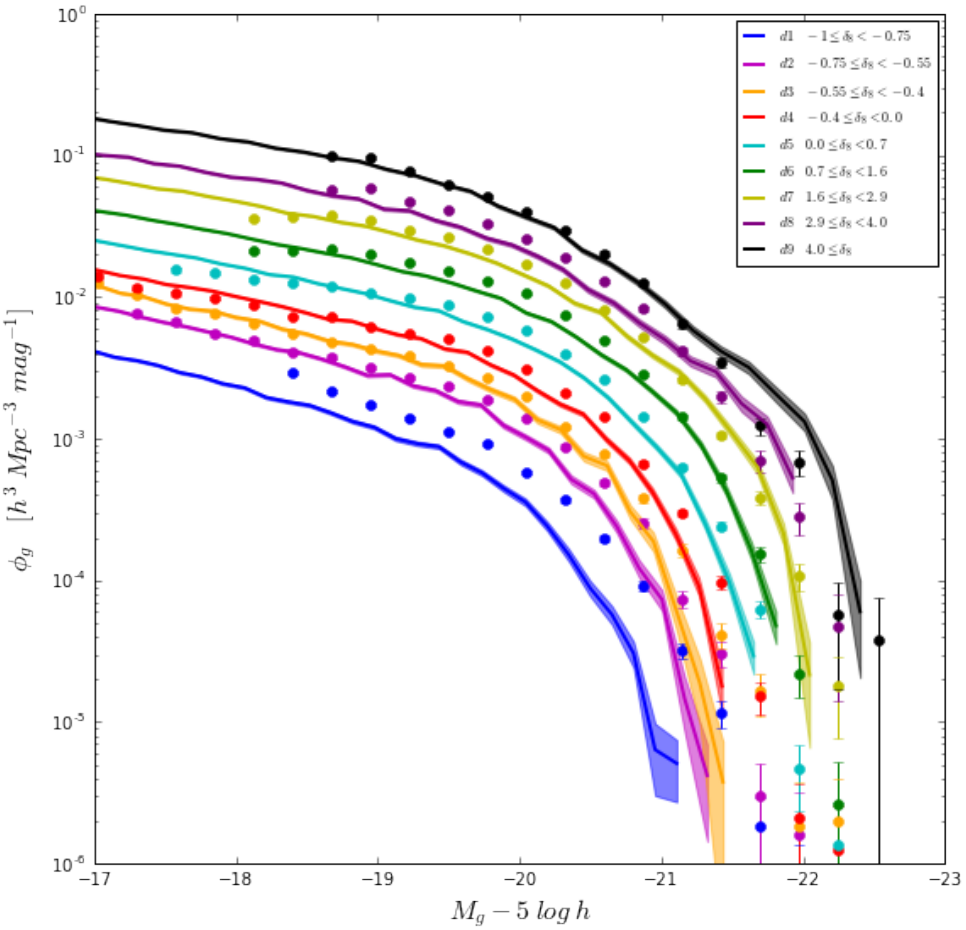

Figure 7: A comparison of BolshoiP mock LFs (solid lines) with SDSS LFs (circle markers) in 9 different density environments on the 8 Mpc scale, using g-band magnitudes.

In a similar manner to the previous figures, Fig. 7 illustrates again the the predicted BolshoiP mock LFs compared to the SDSS LFs using spheres of 8 Mpc but this time in the g-band. There is once again an agreement between the observational data and the mock LF's, though with visibly greater deviations when increasing in brightness than in the r-band.

Figure 8 illustrates the predicted BolshoiP mock LFs compared to the SDSS LFs using spheres of 8 Mpc sphere size, this time in the u-band. A similar correlation between the

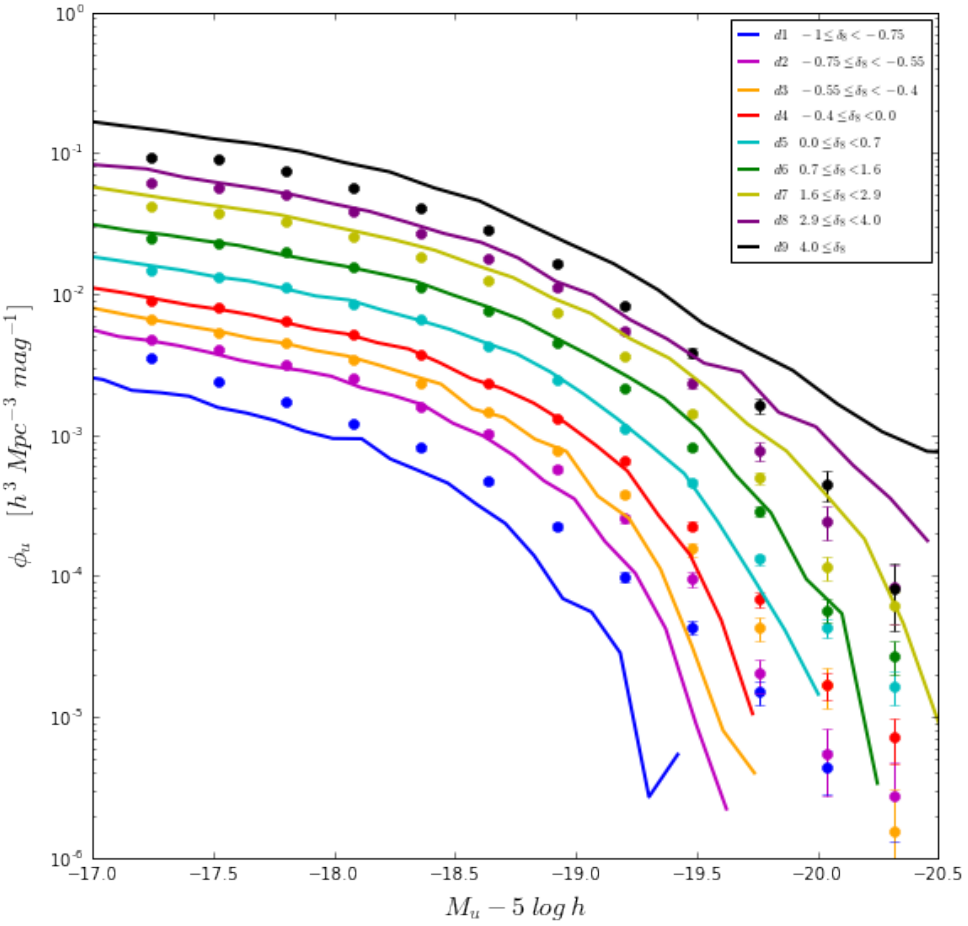

Figure 8: A comparison of BolshoiP mock LFs (solid lines) with SDSS LFs (circle markers) in 9 different density environments on the 8 Mpc scale, using u-band magnitudes.

observational data and the mock LF's are reached at the faint end. However, it appears that there is a deviation between the galaxy-halo connection occurring at the brighter end that is most prominent in the most dense and also in the least dense environments. This outcome was of course an expected result when shifting towards more ultraviolet bands. As mentioned in Section 2.5, observational studies have found that star formation rates has a tendency to correlate with environment. This result is will be important for future studies based on photometric mock data which could lead to wrong results when comparing to observations. Figure 9 shows our predicted BolshoiP mock LFs for the 8 Mpc sphere scale to a different set of observations. Here we compared observations from [9] who used the GAMA survey. The GAMA survey is developed from previous spectroscopic surveys, such as SDSS, the

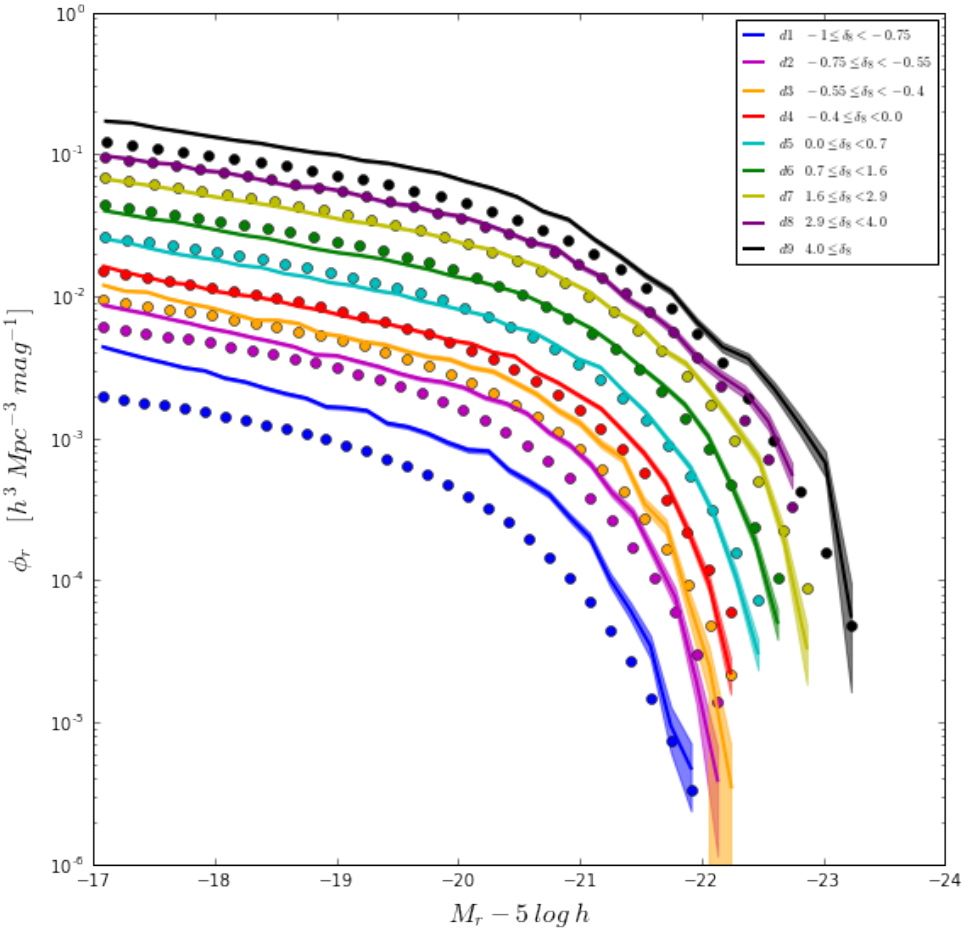

Figure 9: A comparison of BolshoiP mock LFs with GAMA LFs in different density environments on the 8 Mpc scale, using r-band magnitudes.

2dF Galaxy Redshift Survey (2dFGRS) and the Millennium Galaxy Catalogue (MGC). The GAMA team executed this survey by using the AAOmega multi-object spectrograph on the Anglo-Australian Telescope (AAT) and it contains $\sim 300,000$ galaxies of magnitudes of $r < 19.8$ over ~ 286 deg^2. Similarly to the LFs presented from the SDSS, [9] calculated the LFs from the GAMA survey using spheres of 8 Mpc to count neighbors. Here we reproduce their results using Schechter functions (see Eq. 9) with the best fit parameters $\alpha = -1.25$, $\log \phi^* = -2.03$, and $M^* = -20.70$. Again, solid lines are mock LF's and circle markers represent observations. Similarly to Fig. 5, there is a striking resemblance in most density regions with exceptions in the lowest and highest density environments. Note that for the comparison we are using their best fit models to Schechter functions which at the same time

were parameterized as a function of environment. By looking to Fig. 7 in [9] we find that their fits are actually very inaccurate both for at the lowest and highest density bins which explains the disagreement with LFs. Nevertheless, is encouraging that by using two data sets we find that our mock LFs give and accurate description of the observed universe.

4 Summary and Discussion

In this paper we use a photometric mock catalog based the BolshoiP simulation by using abundance matching. To do so, we calculate galaxy luminosity to halo maximum circular velocity relationships in the u, g and r bands. Our main goal was to determine to what extent the validity of the assumption that galaxy luminosity to halo maximum circular velocity relationships is independent of environment. This was motivated by the standard application of this relation where the independency is assumed by default, for which it has been proved that galaxy clustering is in excellent agreement with observed data. While previous studies have found that this is the case when using stellar mass, there are no systematical studies regarding this assumption by using luminosities in different bands. In this paper, we test the above by studying the dependence of the luminosity function with environment and compared to the predictions when the galaxy luminosity to halo maximum circular velocity relation is assumed to be universal based on our photometric mock catalog. The main results and conclusions are:

1. When measuring the environment in spheres of 8 Mpc in the r-band the predicted BolshoiP mock LFs compared to the SDSS LFs are in excellent agreement. Similarly, when comparing to the GAMA LFs instead.

2. When measuring the environment in spheres of 16 Mpc in the r-band we also find that the BolshoiP mock LFs compared to the SDSS LFs are in excellent agreement. Though we caution to the reader that the 16 Mpc scale is not very reliable to probe in underdense and overdense regions because it averages over such a large region.

3. When measuring the environment in spheres of 8 Mpc in the g-band the predicted BolshoiP mock LFs compared to the SDSS LFs are in excellent agreement. Though, this has visibly greater deviations when increasing in brightness than in the r-band.

4. When measuring the environment in spheres of 8 Mpc in the u-band we find a less impressive agreement with observations. It appears that there is a deviation between the galaxy-halo connection occurring at the brighter end that is most prominent in the most dense and also in the least dense environments.

This experiment demonstrates that by using a simple semi-empirical model approach we can obtain remarkable agreement between our simulation and observations, specially when using the r band. The luminosity-halo connection for our observations appear to have a consistent trend. The agreement is best along the knee of the Schechter function for all environments, and is relatively constant across all magnitudes for medium density environments. By inspection, we see that in the lowest environment bin, the observed LF from GAMA is shifted farther below our prediction. This could be due to inadequate fits in [9], as we see in their Fig. 7 the Schechter function parameters deviate the greatest from their fits in underdense environments.

Our main conclusion is that at least in the 8 Mpc scale, there is no dependence on environment for the luminosity-halo connection. This is also evident on the 16 Mpc scale, though the connection is inconclusive for the most overdense regions. Thus, the luminosity-halo connection also seems to be independent to the scale that we investigate, especially in medium density environments. It is apparent that there are no other significant parameters to consider in the luminosity to halo relation. Thus we conclude that assuming a universal luminosity to halo maximum circular velocity relation in the r band is an excellent approximation. The same is true for the g band though we find hints of a small dependence with environment. Finally, we find that assuming a universal relation in u band is not supported by observations. The reason for this is because the u band is more sensible to probe the star formation which is a well established observation that it does depend on environment.

The results presented in this paper are a first step towards the understanding of the galaxy-halo connection, especially due to the traditional assumption that this connection is independent on environment. It is important to note that more work is required in this direction since our experiments were carried out only for 8 and 16 Mpc scales. Is this also true for smaller spheres? Unfortunately, this question is not easy to address in real data and the reason is simple because while simulations have access to the real 3D positions of mock galaxies, in observations we are limited to study galaxies in their redshift space where their peculiar motions introduce an uncertainty in determining their real positions. Nevertheless, simulations can be easily projected into redshift space and thus address the environments at different scales. Alternatively, we can also predict scaling relations that could easily be compared to observations using our 8 Mpc spheres and thus to better understand the galaxy-halo connection, as we will discuss below. Finally, we would like to note, that our result will be important for future studies based on photometric mock data.

4.1 Future Work

As mentioned in the introduction, galaxies form and evolve in dark matter halos. This naturally leads to the assumption that the observed properties of galaxies should be closely related to the properties and evolution of dark matter halos. Indeed, several authors have proposed that properties such as the mass accretion rate of the halos should correlate with the star formation rate of the galaxies and thus with their intrinsic colors [6][12].

Figure 10 shows prediction of medians halo mass accretion rates as a function of the environment by using our 8 Mpc scales as a function of the r band luminosity. Halo mass accretion rates were measured over a period of 100 Myr and also a 1 Tdyn (0.47 Myr) dynamical time scale. For the purpose of obtaining simple correlations with environment, we used six half-integer magnitude bins between -23 and -17. Similarly for Fig. 11 we have five of the same magnitude bins and concentrations on the vertical axis. We see that in the brightest regions the mass accretion rate is highest for the most dense environments, while in

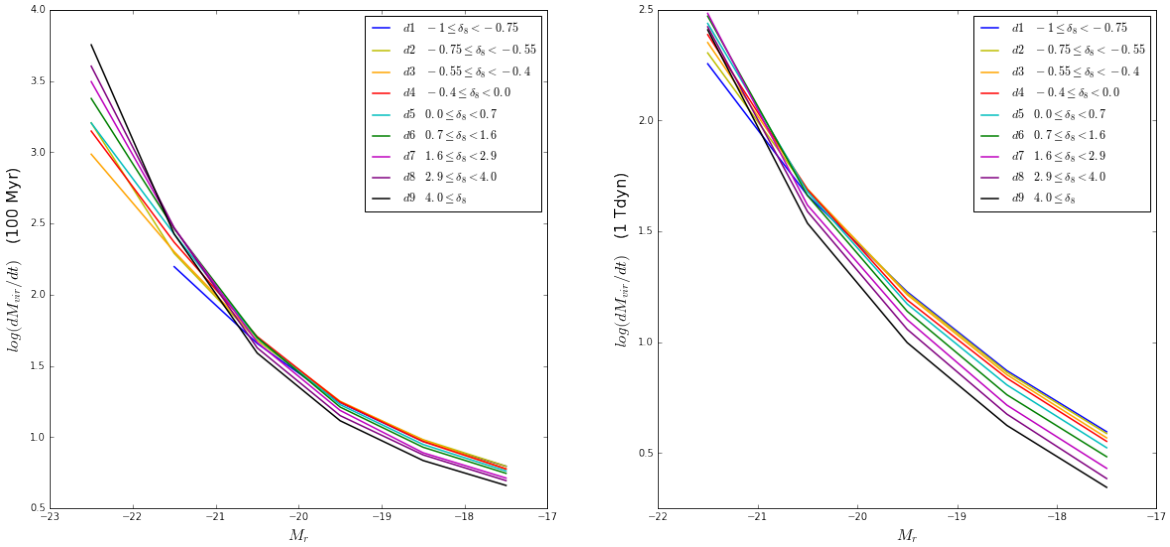

(a) 100 Myr (b) 1 Tdyn

Figure 10: On the x-axis we have red band magnitudes and on the y-axis are mass accretion rates in the a) 100 Myr scale and b)1 Tdyn scale.

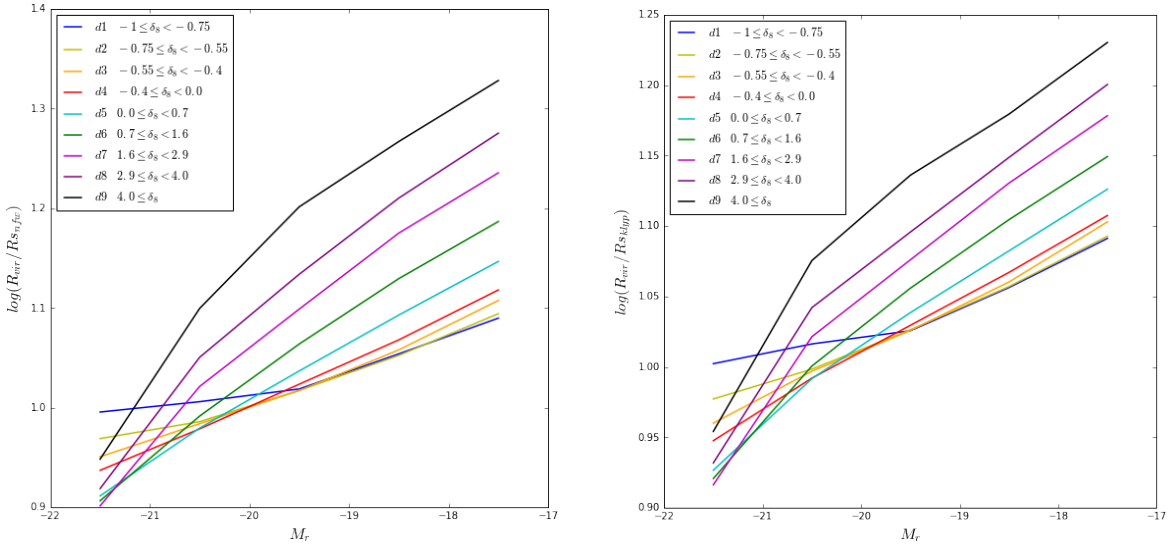

(a) R_{vir}/R_{s-nfw} (b) R_{vir}/R_{s-klyp}

Figure 11: On the x-axis we have red band magnitudes and on the y-axis are concentrations a) with respect to R_{s-nfw} and b)with respect to R_{s-klyp}.

the dimmest regions it is highest in the least dense environments. Dense environments may have the greatest effect on mass accretion rates. We are planning to use these predictions to compare directly with observations in order to introduce an extra constraint for the galaxy halo connection.

Figure 11 shows the same but for the halo concentration parameter (defined as the ratio of the virial radius to the characteristic radius where the logarithm of the slope of halo density is -2). Previous authors have claimed that this parameter should correlate with the age/color of the galaxy [13][14]. The reason for this is that the concentration of the halo is a good proxy for the formation time of the halo [15]. At a fixed halo mass, high concentration halos are older compared to those with low concentrations. Concentrations are shown for two scales of R_s. Here $R_{s,Klyp}$ is an analytic formulae found in [16], while $R_{s,nfw}$ was directly measured in the simulation by assuming that halos are well described by a Navarro-Frenk-White profile. In general, we observe that concentrations correlate with environment very strongly. High concentration halos are in dense environments while low concentration halos are in low environments special for galaxies below $M_r \sim -19$ mag. For brighter magnitudes we see a cross over. Explaining this cross over phenomena is beyond the scope of this paper but we would like to highlight that this makes and strong predictions for future observations. For future work we are planning to compare the predictions shown above to real observations.

5 References

1. Behroozi, Peter S., Risa H. Wechsler, and Charlie Conroy. "The Average Star Formation Histories Of Galaxies In Dark Matter Halos From Z = 0-8." ApJ The Astrophysical Journal 770.1 (2013): 57. Web.

2. Behroozi, Peter S., Risa H. Wechsler, and Hao-Yi Wu. "The Rockstar Phase-Space Temporal Halo Finder And The Velocity Offsets Of Cluster Cores." ApJ The Astrophysical Journal 762.2 (2012): 109. Web.

3. Bryan, Greg L., and Michael L. Norman. "Statistical Properties of X-Ray Clusters: Analytic and Numerical Comparisons." ApJ The Astrophysical Journal 495.1 (1998): 80-99. Web.

4. Avila-Reese, Vladimir. Abundance Matching Technique. Digital image. N.p., n.d. Web.

5. Reddick, Rachel M., Risa H. Wechsler, Jeremy L. Tinker, and Peter S. Behroozi. "The Connection Between Galaxies And Dark Matter Structures In The Local Universe." ApJ The Astrophysical Journal 771.1 (2013): 30. Web.

6. Rodriguez-Puebla A. et al., "Halo and Subhalo Demographics with Planck Cosmological Parameters: Bolshoi-Planck and MultiDark-Planck Simulations." Monthly Notices of the Royal Astronomical Society 1602048113R (2016): n.p. Web.

7. Blanton, Michael R. et al. "New York University Value-Added Galaxy Catalog: A Galaxy Catalog Based on New Public Surveys." Astron J The Astronomical Journal AJ 129.6 (2005): 2562-578. Web.

8. Blanton, Michael R. et al. "The Galaxy Luminosity Function and Luminosity Density at Redshift Z = 0.1." ApJ The Astrophysical Journal 592.2 (2003): 819-38. Web.

9. Mcnaught-Roberts, T. et al., "Galaxy And Mass Assembly (GAMA): The Dependence of the Galaxy Luminosity Function on Environment, Redshift and Colour." Monthly Notices of the Royal Astronomical Society 445.2 (2014): 2125-145. Web.

10. Croton, Darren J. et al., "The 2dF Galaxy Redshift Survey: Luminosity Functions by Density Environment and Galaxy Type." Monthly Notices of the Royal Astronomical Society 356.3 (2005): 1155-167. Web.

11. Blanton, Michael R., and Sam Roweis. "K -Corrections and Filter Transformations in the Ultraviolet, Optical, and Near-Infrared." Astron J The Astronomical Journal AJ 133.2 (2007): 734-54. Web.

12. Dekel, A. et al. "Cold Streams in Early Massive Hot Haloes as the Main Mode of Galaxy Formation." Nature 457.7228 (2009): 451-54. Web.

13. Bullock, J. S. et al. "A Universal Angular Momentum Profile for Galactic Halos." ApJ The Astrophysical Journal 555.1 (2001): 240-57. Web.

14. Hearin, A. P., Watson & D. F. et al. "The Dark Side of Galaxy Colour: Evidence from New SDSS Measurements of Galaxy Clustering and Lensing." Monthly Notices of the Royal Astronomical Society 444.1 (2014): 729-43. Web.

15. Wechsler, Risa H. et al. "Galaxy Formation at Z 3: Constraints from Spatial Clustering." ApJ The Astrophysical Journal 554.1 (2001): 85-103. Web.

16. Klypin, Anatoly A., Sebastian Trujillo-Gomez, and Joel Primack. "Dark Matter Halos In The Standard Cosmological Model: Results From The Bolshoi Simulation." ApJ The Astrophysical Journal 740.2 (2011): 102. Web.